

# An experimental study of diesel engine cam and follower wear with particular reference to the properties of the materials

J. Michalski \*, J. Marszalek, K. Kubiak

*Faculty of Mechanic Engineering and Aeronautics, Rzeszów University of Technology, 35-959 Rzeszów, ul. W. Pola 2, Poland*

Received 9 August 1999; received in revised form 17 February 2000; accepted 17 February 2000

## Abstract

The main objective of this paper is to study and experimentally quantify the cam and follower wear mechanisms of a diesel direct valve-gear. Camshafts are made of nodular cast iron, surface hardened, ion nitrided and nitrosulphurized, and those made of grey chilled cast iron are mated with followers made of chilled grey cast iron and hardened steel. The investigation was carried out on a laboratory bench equipped with an engine head with a camshaft, followers and systems creating the conditions necessary for a routine run of the valve gear. Cam wear was defined by comparing the profile lifts of the cams. The height of the followers was measured using a coordinative measuring machine and a perpendicular optimizer. The rotational speed, valve displacement and the torque required by the valve gear were measured. Camshaft C9 and the thimble shaped followers with regulating plates F6 were also examined in a diesel engine. The effects of the materials the kinematic pair was made of, heat treatment and thermochemical treatment, the cams' own stresses at the moment-of-friction value, as well as the extent and nature of element wear, were analysed. © 2000 Elsevier Science S.A. All rights reserved.

*Keywords:* Wear mechanism; Cams and followers; Diesel engine; Properties of the materials

## 1. Introduction

A cam–follower kinematic pair works under complicated conditions of mechanical load, and wears during operation. The contact surfaces of the cam and the follower are usually surface hardened. The hardening may be due to phase transformation or precipitation processes occurring in the material during heat treatment or thermochemical treatment.

## 2. Review of the literature on the valve shaft cam and follower wear

With respect to the geometry and kinematics of combustion engine valve gear, it is generally assumed that the value of Hertzian pressure has a direct effect on the pitting

wear value [1]. It often concerns cams mating with a roller follower [2] where the wear may be increased, particularly due to the occurrence and propagation of cracks.

It follows from a previous investigation [3] that an increase in the valve spring strength by 310 N for cams made of 38–42 HRC chilled cast iron mating with 50–52 HRC chilled cast iron plates after  $3 \cdot 10^6$  revolutions of 900 r.p.m., increased the wear of the cam lobe by 9  $\mu\text{m}$  after 56 h and the attack and taper sides by about 12  $\mu\text{m}$ .

Pitting most often occurs in a follower type timing gear system with the camshaft inside the engine block. Scuffing (seizing caused by breaking through the oil film) or scoring (scratches in the surface) are typical kinds of cam–follower wear [4]. Most methods of scuffing investigation concern an engine with OHC-overhead camshafts. Attrition is also a typical kind of cam and follower wear. It results from a considerable oil viscosity change in the cam–follower contact area due to both load and temperature change. The thickness of the oil film is too small to ideally separate all the irregularities of the mating surfaces [5]. It may lead to welding and breaking of the connections between the peaks of the irregularities in the contact

\* Corresponding author.

microareas. Those conditions are usually aggravated by attrition, plastic deformation and adhesion wear [6].

The most often mentioned factors affecting the cam–follower wear are the materials the mating elements are made of, rotational speed, the dynamics of the camshaft–follower kinematic pair, the temperature and viscosity of the oil and operational conditions [7,8].

Most often, the face of the follower shows even wear over the whole area, and greater wear values sometimes occur in the central area. It particularly refers to abrasive wear due to pitting or scuffing. If scuffing is responsible for intensive wear, higher wear values occur on the side of the follower face or the wear process becomes more complicated [6].

### 3. Materials used for camshafts and followers

Chilled grey cast iron is commonly used worldwide for camshaft production. The inclusion of that material in the 1966–1970 production was estimated at 32–55% [9]. The percentage of camshafts made of steel and surface hardened grey cast iron, nodular cast iron and malleable cast iron was 21–29%, 11% and 7%, respectively.

The durability and reliability of the valve-gear depend not only on what the camshaft is made of but also on the material properties of the camshaft–follower pair. The preferred material for a camshaft mating with a slide cam follower at a crane and indirect valve drive is grey metalurgically hardened cast iron [10,11]. It has the following composition: 3.1–3.5% C, 1.8–2.5% Si, max. 0.15% S, max. 0.2% P, 0.5–0.8% Mn, 0.15–0.25% Ni, 0.7–1% Cu, 0.15–0.25% Mo, the rest is Fe. The cam surface gets hardened during primary crystallization. The minimum hardness should be 45 HRC with a 3-mm hardened layer at the lobe and the flanks. Considering the possibility of a camshaft crack, especially during assembly and stripping, the core tensile strength should be at least 235 MPa, at a hardness of 240–300 HB. In such camshafts the cranks are not chilled. The cast iron microstructure just below the surface area should contain transformed ledeburite without graphite. The mating follower should be made of chilled cast iron, hardened and tempered, with an increased content of Ni, Cr, Mo, V. It has the following composition: 3–3.6% C, 2–2.8% Si, max. 0.12% S, max. 0.25% P, 0.4–1% Mn, 0.4–0.7% Ni, 0.9–1.25% Cr, 0.4–0.7% Mo, the rest was Fe. The minimum hardness of the follower should be 54 HRC with the depth of the hardened layer being 3 mm. Such a material pair is particularly recommended for heavy duty diesel engines.

The material recommended for a camshaft of a direct valve drive mating with a slide follower is also chilled cast iron. However, in this respect, the follower, in view of the necessary great strength and rigidity, combined with a small mass indispensable at great speeds, should have a

light skeleton structure and be made of steel. The face of the follower is carburized down to 0.3 mm and hardened up to 59–63 HRC. The strength of the follower core is 1000 MPa and its hardness 310–380 HB.

Cams mating with regulating plates resting in the nest of the thimble-shaped follower and with a hydraulic follower are used for direct valve drive. Followers are also made of chilled cast iron, hardened and tempered. However, a camshaft for a hydraulic follower must have an extra chilled profile core surface of the cam.

Next, for a roller follower, the camshaft should be made of steel composite [12] or steel, most often with induction hardened cams to a depth of at least 1 mm, up to 60–64 HRC. The roller is made of steel carburized to a minimum depth of 0.8 mm and hardened up to 60–64 HRC. The roller is often made of hardened and low tempered steel.

Very often, camshafts and followers are subjected to thermo-chemical treatment. It is most frequently ion nitriding, oxidation, phosphatizing, sulphurizing or spraying on of multicomponent layers. At present, camshafts with chilled cams are made using the upper surface remelting method. It is usually done with an electric arc (TIG method) and rarely with laser light or an electron beam [13]. Much research work is also being done on the application of technological ceramics, hard sintered metals and composites [12,14,15].

It was found that the kind of finishing touch machining of shaft cams and the follower face has a crucial effect on the wear of the mating elements [16]. Traditional grinding is being replaced by the abrasive honing of shaft cams, preferably of plateau structure, as well as the lapping and polishing of the follower face. The occurrence of negative internal stresses after such work is of vital importance. The application of such technology for grey chilled cast iron cams mating with a follower made of grey isothermally hardened and tempered cast iron made it possible, under the same conditions, to reduce cam wear on average by 4  $\mu\text{m}$  and the follower face wear by 1.5  $\mu\text{m}$  in relation to those surfaces subjected only to grinding [8].

### 4. Programme and research conditions

The investigation focused on the effect of cam and follower materials and their thermal and thermochemical treatment on cam and follower functional properties.

The elements of the valve gear are shown in Fig. 1. During the combustion engine operation, the cam of the camshaft mating with the follower of the direct valve gear is under the load of valve springs  $P_s$ , force of inertia  $P_b$ , friction forces  $T_1, T_2, T_3, T_4, T_5, T_6$ , gas force or the force of the rest of exhaust fumes  $P_g$  (Fig. 1). Axial friction forces put extra load on the attack flank of the cam and release the taper flank. The forces are due to the friction of the bottle against the valve guide surface in head  $T_5$  as

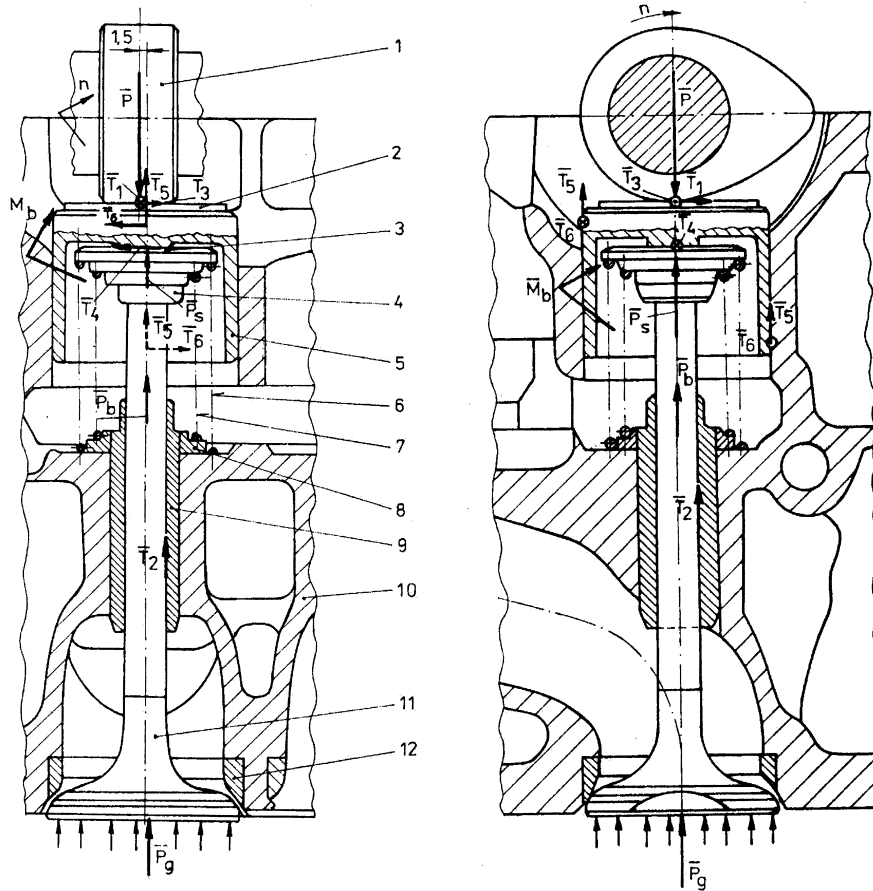


Fig. 1. Elements of valve gear with forces and moments. 1 — cam, 2 — cam follower (construction variant consisting of a bottle and tappet), 3 — valve key, 4 — upper valve spring cup, 5 — bottle, 6 — outer spring, 7 — inner spring, 8 — lower cup of valve spring, 9 — valve guide, 10 — engine head case, 11 — valve, 12 — valve seat,  $M_b$  — moment of inertia,  $P_b$  — force of inertia,  $P_g$  — gas force,  $P_s$  — spring force,  $P$  — resultant force,  $T_1, T_2, T_3, T_4, T_5, T_6$  — friction forces.

well as the friction of the valve stem against valve guide  $T_2$ . The circumferential friction forces result from the shift of the cam axis from that of the follower. Force  $T_1$  causes the rotation of the follower together with its bottle. The friction of the follower against the cam due to its rotation  $T_3$ , the friction of the bottle against head  $T_6$  as well as against the face of the  $T_4$  valve stem, also occur.

The investigation was carried out on a laboratory bench equipped with an engine head with a camshaft, followers and systems creating the conditions necessary for a routine run of the valve gear. The main details of the experimental apparatus are presented in Fig. 2. The test conditions were worked out as a basis using the procedure of checking the oil usability to counteract the wear of valve gear elements [17]. The so called “cold” test phase, at  $40 \pm 10^\circ\text{C}$  oil temperature, lasted for 40 h ( $1.7 \times 10^6$  revolutions) at a camshaft speed of 750 r.p.m. The hot test phase, at  $100 \pm 10^\circ\text{C}$  oil temperature, lasted for about 60 h ( $5.4 \times 10^6$  revolutions) at 1500 r.p.m. An electric motor, not a combustion one, with a possibility of controlling and stabilizing the rotational speed was used to drive the camshaft. The filtering and oil lubrication systems were comparable

to those of a combustion engine. A diesel CD class engine mineral oil of 15W40 viscosity was used for the test.

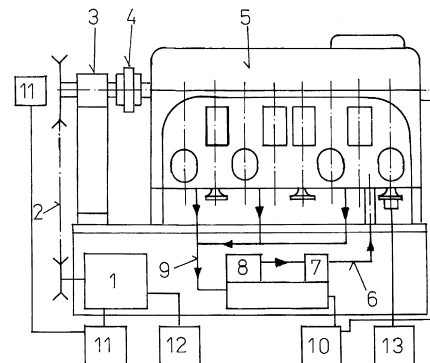


Fig. 2. Bench for checking cam and follower wear. 1 — electric motor, 2 — belt transmission, 3 — shaft power unit, 4 — flexible coupling, 5 — engine head with camshaft, followers and valves, 6 — lubricating oil pipe, 7 — oil filter, 8 — oil pump with overflow valve and electric motor, 9 — lubricating oil outlet pipe, 10 — control and stability system of lubricating oil temperature, 11 — measurement, control and stability system of shaft rotational speed, 12 — power measurement system, 13 — system of measurement and analysis of amplitude, speed and acceleration.

Table 1  
Metallographic characterization of the camshafts under investigation

| Cam-shaft       | Chemical composition, % |      |      |      |      |      |      |      |      | Mean hardness<br>of the cams | Hardness of the<br>cam-shaft core | Thickness of<br>lobe hardening | Method of hardening<br>the cams <sup>a</sup> |
|-----------------|-------------------------|------|------|------|------|------|------|------|------|------------------------------|-----------------------------------|--------------------------------|--|
|                 | C                       | Si   | Mn   | P    | S    | Cr   | Ni   | Mg   | Cu   |                              |                                   |                                |  |
| C1              | 3.42                    | 2.20 | 0.56 | 0.04 | 0.01 | –    | 0.90 | 0.06 | –    | 53 HRC                       | 270                               | 5                              | HP   |
| C2              | 3.44                    | 2.15 | 0.60 | 0.05 | 0.01 | –    | 0.95 | 0.05 | –    | 55 HRC                       | 275                               | 13                             | HP   |
| C3              | 3.42                    | 2.20 | 0.65 | 0.05 | 0.01 | –    | –    | 0.06 | 0.80 | 587 HV1                      | 280                               | 0.01                           | AJ   |
| C4              | 3.41                    | 2.10 | 0.70 | 0.06 | 0.01 | –    | –    | 0.05 | 0.80 | 443 HV1                      | 290                               | 0.01                           | AS   |
| C5              | 3.44                    | 2.21 | 0.58 | 0.04 | 0.01 | –    | 0.90 | 0.06 | –    | 587 HV1                      | 274                               | 0.01                           | HP, AJ                                       |
| C6              | 3.47                    | 2.24 | 0.62 | 0.05 | 0.01 | –    | 0.85 | 0.05 | –    | 443 HV1                      | 275                               | 5.5                            | HP, AS                                       |
|                 |                         |      |      |      |      |      |      |      |      |                              |                                   | 0.01                           |  |
|                 |                         |      |      |      |      |      |      |      |      |                              |                                   | 5.5                            |  |
| C7              | 3.60                    | 1.82 | 0.68 | 0.16 | 0.03 | 0.20 | –    | –    | –    | 47 HRC                       | 270                               | 15                             | Z  |
| C8              | 3.44                    | 2.15 | 0.61 | 0.05 | 0.01 | 0.64 | 0.80 | –    | –    | 51 HRC                       | 280                               | 12                             | Z  |
| C9 <sup>b</sup> | 3.40                    | 2.10 | 0.60 | 0.05 | 0.01 | 0.61 | 0.80 | –    | –    | 51 HRC                       | 280                               | 12                             | Z  |

<sup>a</sup>HP — surface hardening, AJ — ion nitriding, AS — sulfonitriding, Z — chilling.

<sup>b</sup>1000-h engine test.

Table 2  
Metallographic characterization of the followers under investigation

| Notation        | Chemical composition, % |      |      |      |      |      |     |     |      |      | Face hardness | Thickness of the hardened layer | Method of hardening <sup>a</sup> |
|-----------------|-------------------------|------|------|------|------|------|-----|-----|------|------|---------------|---------------------------------|----------------------------------|
|                 | C                       | Si   | Mn   | P    | S    | Cr   | Ni  | Mo  | Ti   | V    |               |                                 |                                  |
| F1              | 3.50                    | 2.25 | 0.78 | 0.13 | 0.09 | 0.40 | 1.4 | 0.7 | 0.03 | 0.15 | 60            | 5                               | Z                                |
| F2              | 3.40                    | 2.35 | 0.75 | 0.14 | 0.10 | 0.35 | 1.3 | 0.6 | 0.03 | 0.12 | 61            | 5                               | Z                                |
| F3              | 3.60                    | 2.35 | 1.00 | 0.15 | 0.07 | 0.60 | 1.7 | 0.7 | 0.03 | 0.20 | 63            | 7                               | Z                                |
| F4              | 3.50                    | 2.30 | 0.90 | 0.15 | 0.09 | 0.55 | 1.5 | 0.6 | 0.03 | 0.15 | 58            | 4                               | Z, H                             |
| F5              | 0.37                    | 0.22 | 0.86 | –    | 0.01 | 0.89 | –   | –   | –    | –    | 59            | 2                               | HP                               |
| F6 <sup>b</sup> | 0.38                    | 0.20 | 0.86 | –    | 0.01 | 0.85 | –   | –   | –    | –    | 59            | 2                               | HP                               |

<sup>a</sup>Z — chilling, H — hardening, HP — surface hardening.

<sup>b</sup>1000-h engine test.

Physical properties of the applied oil were the following: absolute viscosity at 40°C, 119 mPa s; absolute viscosity at 100°C, 14.4 mPa s; viscosity index 130, freezing point –24°C, kindling temperature 210°C, base number 10 mg KOH/g, density 882 kg/m<sup>3</sup>. A mercury and electric thermometers made it possible to measure the oil temperature and regulate it automatically. The rotational speed, valve displacement and the torque required by the valve gear were measured.

Camshaft C9 (Tables 1 and 2) and the thimble shaped followers with regulating plates F6 (Table 2) were also examined in a diesel engine. The running-in of the engine and its reliability tests were carried out at a bench equipped with an eddy-current dynamometer. The total time of the shortened running-in according to the Polish standard was 30 h [18]. In 11 consecutive stages, the rotational speed of the crankshaft increased gradually from 800 to 5200 r.p.m. The torque was gradually increased until it reached the final value at maximum power. The 1000-h long reliability tests were carried out in 3-h cycles [19]. Each cycle consisted of eight stages. Each stage comprised the following successive sub-stages: running the engine at 800 r.p.m. and no external load, at 3500 r.p.m. at maximum torque and at 5200 r.p.m. at maximum power torque.

The examined elements had material properties identical to those of the C8 and F5 elements tested in the engine head in the laboratory bench. Cam wear was defined by comparing the profile lifts of the cams. The measurement was carried out using the plunger ball end of a coordinative measuring machine and, additionally, on an optical dividing head using a flat end. The height of the followers was also measured using a coordinative measuring machine and a perpendicular optimeter. The internal stresses of the cams and the volume of the retained austenite were determined by the X-ray method. The layer of the material was electrolytically removed. The stresses were measured perpendicularly to the camshaft axis by the  $\sin^2 \psi$  method. The cams had a synthetic profile and a 9-mm travel. The maximum speeds of the lost slide motion were 3 and 4.2 m/s. The resultant forces exerting load on the kinematic pair are, at 1500 rev/min, 600 N at the lobe and 1150 N at the flanks of the cams. This produces a Hertzian unit pressure equal to 425 MPa at the lobe and 250 MPa at the flanks. The heights of the irregularities of the ground surfaces of the cams and the follower faces were  $R_a = 0.56\text{--}0.80 \mu\text{m}$  and  $R_a = 0.35\text{--}0.47 \mu\text{m}$ , respectively. After ion nitriding, the approximate height increased to  $R_a = 0.74\text{--}1.15 \mu\text{m}$ . The approximate height value for sulfoni-

Table 3  
Material characterization of the camshafts under investigation and their hardened layer

| C1  | C2  | C3  | C4   | C5   | C6  | C7  | C8, C9 <sup>a</sup>    |
|---|---|---|--|--|---|---|------------------------|
| nodular pearlitic cast iron   | nodular pearlitic cast iron   | pearlito-ferritic nodular cast iron   | pearlito-ferritic nodular cast iron                                    | pearlite nodular cast iron   | pearlite nodular cast iron  | grey cast iron                            | chromic grey cast iron |
| fine-acicular martensite, ferrite 5%, retained austenite 5%, nodular graphite | acicular martensite, ferrite 5%, retained austenite 12%, nodular graphite | diffusion nitrided layer phase $\epsilon$ , pearlite, nodular graphite, ferrite 20% | sulfanitrided diffusion layer, pearlite, nodular graphite, ferrite 20% | diffusion nitrided layer phase $\epsilon$ , tempered martensite, bainite, nodular graphite | sulfanitrided diffusion layer, tempered martensite, bainite, nodular graphite | converted ledeburite, cementite, pearlite | converted ledeburite   |

<sup>a</sup>1000-h engine test.

trided surfaces was  $R_a = 0.32\text{--}0.46 \mu\text{m}$ . The thermal and thermochemical treatment followed the routine typical of those elements.

## 5. Investigation results

Camshafts of nodular cast iron and of grey cast iron were denoted with symbols ranging from C1 to C8. Their chemical composition and technical characterization are presented in Table 1. A similar presentation of characteristics for followers F1–F5 is given in Table 2. The microstructures of the kinematic pairs under investigation are shown in Tables 3 and 4. The tribologic wear values for those pairs are listed in Table 5. The interval stress values in the surface area of the cams and the moment of frictional resistances were also presented. Figs. 3–5 show the characteristic microstructures and the fractographic examination results. A light microscope and matrix replicas were used. Subsequently, Fig. 6 shows the distribution of internal stresses, the volumes of retained austenite and the hardness values as a function of the depth of the hardened layer for cams C1 and C2.

### 5.1. Analysis of investigation results for nodular cast iron camshafts and mating followers

Camshafts C1 and C6 were cast of nodular and pearlitic cast iron (Table 1). The pearlite in the matrix has a fine plate structure. In addition, there occur rare, small grains of free ferrite in the metallic matrix. The surface layers of cams C1, C2, C5 and C6 were hardened inductively and have a hardness typical of that material, i.e. 52–55 HRC. The hardened layers of camshafts C1, C5 and C6 are similar. They are quite different from those of camshaft C2.

#### 5.1.1. Cams of martensite–bainite structure with a varied amount of retained austenite

The particular cams of camshafts C1 and C2 differed noticeably in the thickness of the hardened layer which was equal to 5 and 13 mm, respectively. At the attack and taper sides of the cam, they were 2 and 6 mm, respec-

tively. Detailed investigation has shown that cams of greater hardened depth were strongly overheated and had an increased (about 12%) retained austenite content. Cams of smaller thickness contained 5% retained austenite. Internal stresses near the surface were negative and of similar value (Fig. 7a). However, camshaft C1 had a negative internal stress to a depth of 0.18 mm. On the other hand, camshaft C2, at about 0.04 mm depth, attained zero stress changing into positive stress of 480 MPa at a depth of 0.08 mm. The microstructure of camshaft C1 is fine-acicular martensite with nodular graphite (Fig. 8b). In the transitory layer, martensite is transformed into bainite. Camshaft C2 has a microstructure composed of acicular martensite and nodular graphite (Fig. 4). The cams of camshaft C1, mating with follower F1, show smooth abrasive wear on the flanks. In the lobe part of the metal, there occurs the same deep surface cracks, formed perpendicularly to the slide direction (Fig. 8c,d). The maximum value of the lobe wear is 0.022 mm. On the other hand, the flank surfaces of the cams of camshaft C2 mating with follower F2 show numerous large and deep cracks in the surface layer metal. They run more or less perpendicularly to the direction of the sliding on the follower surface (Fig. 4c). In the lobe part, cams C2 have numerous cavities due to metal chipping (Fig. 4d). The maximum value of the lobe wear is 1.022 mm. Although the wear values of cams C1 and C2 differ considerably (Table 5), their wear mechanisms are similar despite a considerable difference in intensity. Cam C1 wore abrasively (Fig. 8c,d). Cam C2 wore by surface cracking and peeling (Fig. 4c,d). The resistances due to the friction of cams C2 against followers F2 were greater too (Table 5).

Followers F1, F2, F3 and F4 were made of cast iron and flake graphite. Due to fast cooling, the cast iron of the follower heads crystallized as white and then was hardened. It ensured a hardness of 58–63 HRC (Table 2). The side surfaces of the followers crystallized as grey cast iron with flake, fine graphite, with a matrix which underwent hardening (bainite). The faces of followers F1 and F2 wore differently. When performing characteristic rotary motion, follower F1 showed even, circumferential, abrasive wear (Fig. 3a,b). Follower F2 showed no traces of rotary work and its face was chipped (Fig. 5a). The microstructure of the facial metal shows a number of

Table 4  
Material characterization of the examined followers and their hardened layer

| F1                     | F2  | F3                          | F4                                  | F5, F6 <sup>a</sup>                 |
|------------------------|---|-----------------------------|-------------------------------------|-------------------------------------|
| Grey chilled cast iron | grey chilled cast iron  | grey chilled cast iron      | grey chilled and hardened cast iron | steel                               |
| Transformed ledeburite | transformed ledeburite, torn off metal fragments, broken cementite plates | fine transformed ledeburite | cementite, martensite, bainite      | without nitriding layer, martensite |

<sup>a</sup>1000-h engine test.

Table 5  
Internal stress values and tribologic characterization of cam–follower pairs

| The kind of kinematic cam–follower pair | Internal, close-to–surface stresses, interval of variability (MPa) | Friction moment, interval of variability (Nm) | Follower maximum wear value, interval of variability (mm) | Cam lobe maximum wear value, interval of variability (mm) | Cam flank maximum wear value, interval of variability (Mm) |
|---|--|---|---|---|--|
| C1–F1                                   | $-570 \pm 37$  | $24 \pm 5$                                    | $0.012 \pm 0.005$   | $0.024 \pm 0.005$   | $0.017 \pm 0.004$  |
| C2–F2                                   | $-450 \pm 16$  | $29 \pm 7$                                    | $0.184 \pm 0.040$   | $1.022 \pm 0.310$   | $0.022 \pm 0.007$  |
| C3–F3                                   | $-600 \pm 40$  | $21 \pm 5$                                    | $0.120 \pm 0.002$   | $0.420 \pm 0.060$   | $0.047 \pm 0.014$  |
| C4–F3                                   | $-120 \pm 12$  | $18 \pm 6$                                    | $0.175 \pm 0.040$   | $1.350 \pm 0.400$   | $0.055 \pm 0.019$  |
| C5–F3                                   | $-700 \pm 47$  | $16 \pm 4$                                    | $0.020 \pm 0.010$   | $0.015 \pm 0.004$   | $0.013 \pm 0.005$  |
| C6–F3                                   | $-220 \pm 22$  | $12 \pm 3$                                    | $0.040 \pm 0.008$   | $0.095 \pm 0.020$   | $0.035 \pm 0.013$  |
| C7–F4                                   | $-530 \pm 39$  | $17 \pm 4$                                    | $0.080 \pm 0.013$   | $0.034 \pm 0.008$   | $0.025 \pm 0.008$  |
| C8–F5                                   | $-650 \pm 47$  | $8 \pm 2$                                     | $0.003 \pm 0.002$   | $0.012 \pm 0.004$   | $0.007 \pm 0.003$  |
| C9–F6                                   | $-655 \pm 52$  | –   | $0.007 \pm 0.004$   | $0.042 \pm 0.006$   | $0.015 \pm 0.005$  |

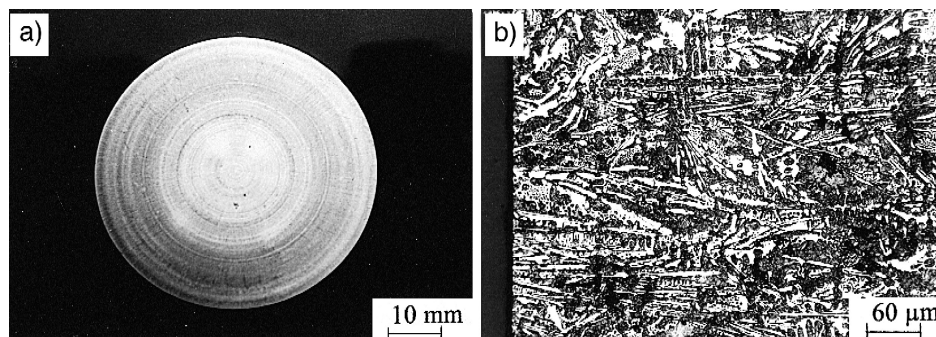


Fig. 3. Follower F1. Macrograph of the face surface (a), microstructure of the surface layer-transformed ledeburite (b).

tear-outs and some delamination wear on the surface and the cementite plates were broken (Fig. 5b). The typical shapes of cams C2 and C1 also show that after wear, the attack side wore more than the taper one (Fig. 9).

#### 5.1.2. Cams of pearlite–ferrite or martensite–bainite base with a layer formed by ion nitriding or nitrosulfurizing

Camshaft C5 was ion nitrided and camshaft C6 was submitted to sulfonitriding by diffusion. Camshafts C3 and C4 were subjected to the same thermochemical treatment as camshafts C5 and C6 but they were not induction hardened. The camshafts were mated with F3 followers

(Table 2). Sulfonitriding was carried out in a soaking furnace with ammonia and sulphur. The thin diffusion layer obtained after nitriding and, first of all, after sulfonitriding dramatically reduces the frictional resistance of the cam–follower kinematic pair (Table 5). The hardness of the surface layer obtained after short nitriding has an average value of 587 HV1. The hardness was considerable, from 401 to 742 HV1, although the measurements were taken on a metal matrix. The thickness of the diffusion zone of phase  $\epsilon$  did not exceed 10  $\mu\text{m}$ . The internal stresses were of negative value,  $-700$ – $-600$  MPa (Table 5). The hardness of the sulfonitrided layer is a bit smaller and equal to 405 HV1 (321–533 HV1). Its thickness is

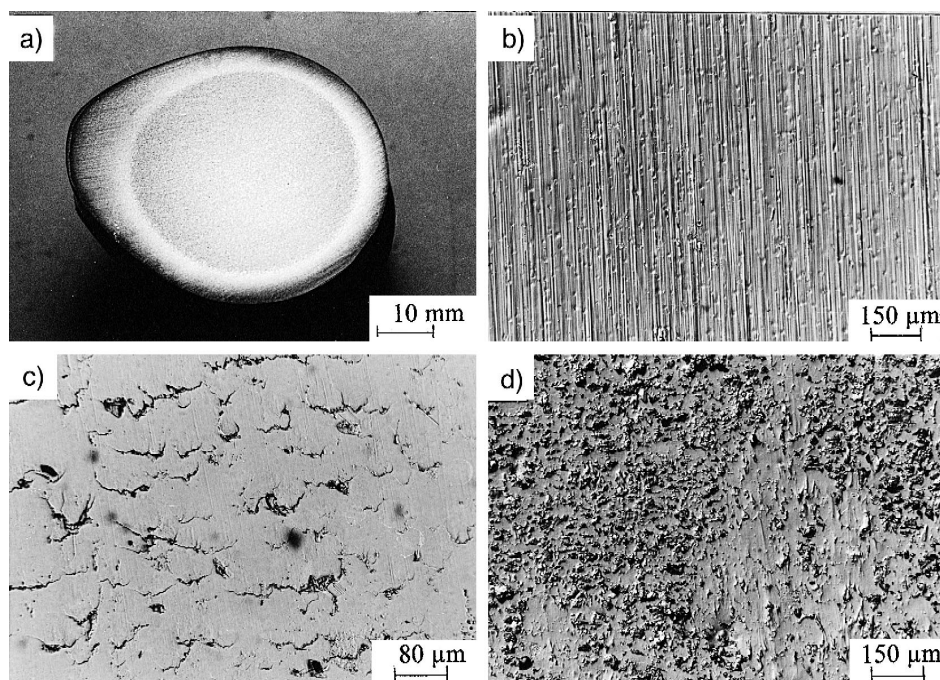


Fig. 4. Cam C2. Crosssection with a dark layer hardened on the circumference (a), the surface of a grinding cam (b), numerous cracks in the cam flank perpendicular to the direction of the slide on the follower face (c), numerous scaling cavities in the metal near the lobe of the cam (d).

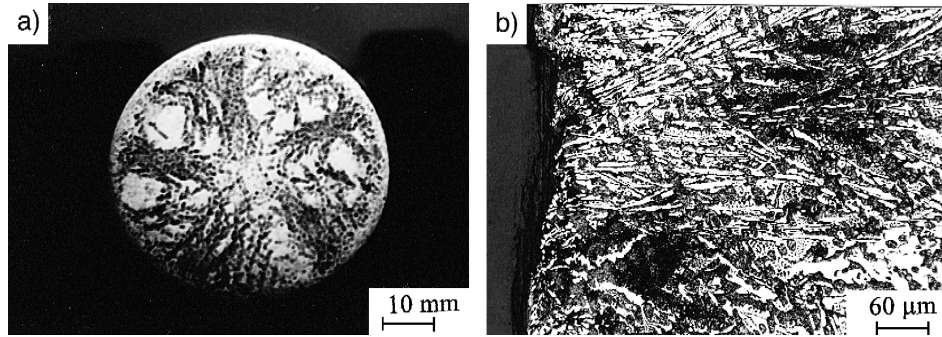


Fig. 5. Follower F2. Macrophotography of the face surface (a), microstructure of the surface layer-transformed ledeburite, separated metal fragments, broken cementite plates (b).

similar to that of the nitrided layer. However, the stresses have a much smaller negative value, i.e.  $-120$ – $-220$  MPa. Irrespective of the base, which was either ferrite-pearlitic or martensitobainitic, the diffusion layers, both nitrided and sulfonitrided, are very uneven, heterogeneous, do not stick to the base very well and are weakened by the release of nodular graphite (Fig. 6b). In the case of cams C3 and C4, up to 20% ferrite was identified, which proves the occurrence of the graphitization process during the thermochemical treatment. The cams of camshafts C3 and particularly C4 show a very extensive lobe wear, i.e. 0.420–1.350 mm. The diffusion layer cracks begin in the

graphite phase (Fig. 6d). The process of microcracking under the scaled surface is of similar nature (Fig. 6c). It should be assumed that the pattern of graphite phases may also be a place where cracks occur and surface scaling begins.

The formation of a nitrided layer on the hard and thick martensitobainitic matrix of cams C5 ensures its small radial wear (Table 5). The cam undergoes smooth abrasive wear (Fig. 6a). Follower F3 also undergoes smooth abrasive wear of a small value. The application of sulfonitriding is not recommended because of the increased wear on the cam and follower despite smaller resistance to motion

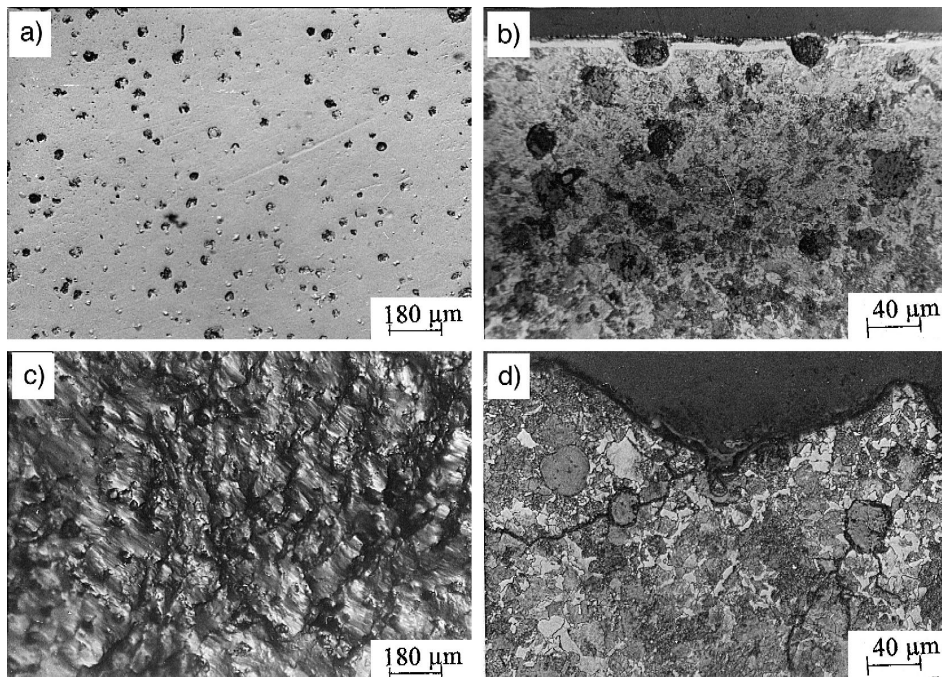


Fig. 6. Cams C4 and C5. Smooth worn surface of shaft C5 after  $0.8 \cdot 10^6$  revolutions (a), ion nitrided diffusion layer of shaft C5 together with pearlite, ferrite and nodular graphite structures after  $0.8 \cdot 10^6$  revolutions (b), scaled C4 shaft surface after sulfonitriding together with pearlite, ferrite and nodular graphite structures (c), down-to-the base cracks propagating from the scaled C4 shaft surface after sulfonitriding (d).

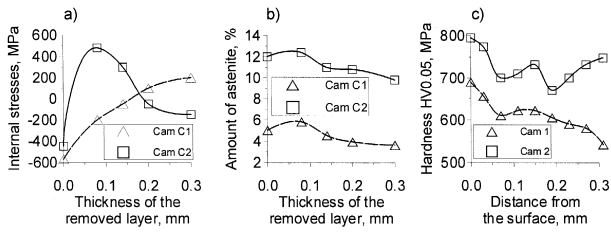


Fig. 7. Change in internal stress (a), participation of retained austenite (b), microhardness (c) in the function of the distance from the surfaces of cams C1 and C2.

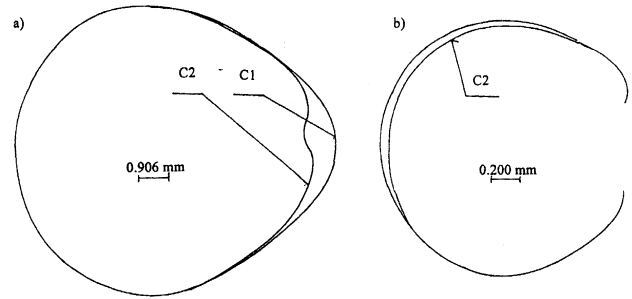


Fig. 9. Outlines of worn out C1 and C2 cams (a), outlines of a fragment of a worn out C2 cam with its outline before the lift test (b).

(Table 5). The wear on the cam is of fatigue nature manifested as numerous surface cracks. The impression of the surface was similar to that shown in Fig. 6c,d.

5.2. Analysis of investigation results for grey cast iron camshafts and mating followers

5.2.1. Chilled cams of transformed ledeburite, cementite and pearlite structure — cam followers of martensite and cementite structure

The valve shaft was made of C7 grey pearlite low-alloyed cast iron. The core was 270 HB and has a pearlite cast iron structure with flake graphite and free carbides which precipitated at the borders of eutectic cells to form a cementite network. The cams were chilled using external

chills. The microstructure of this part of the cam consists of transformed ledeburite: cementite crystals and pearlite grains. The hardness of the cam surface is 0.4–1 HRC. Follower F4 was made of chilled and hardened grey cast iron. The hardness of its face surface is 58–59 HRC. The microstructure is martensite and cementite. Cam C7 shows smooth abrasive wear on the flanks (great surface smoothness) and has small carbide peelings. Its lobe shows great abrasive wear and has a few cavities after chipped hard particles (cementite) and considerable cavities after the separation of large flakes of metal (Fig. 10a). Follower F4 has an evenly worn face surface with small cavities caused by chipped cementite particles and large, groove shaped cavities which might have been caused by hard particles torn out of the cam surface (Fig. 10b).

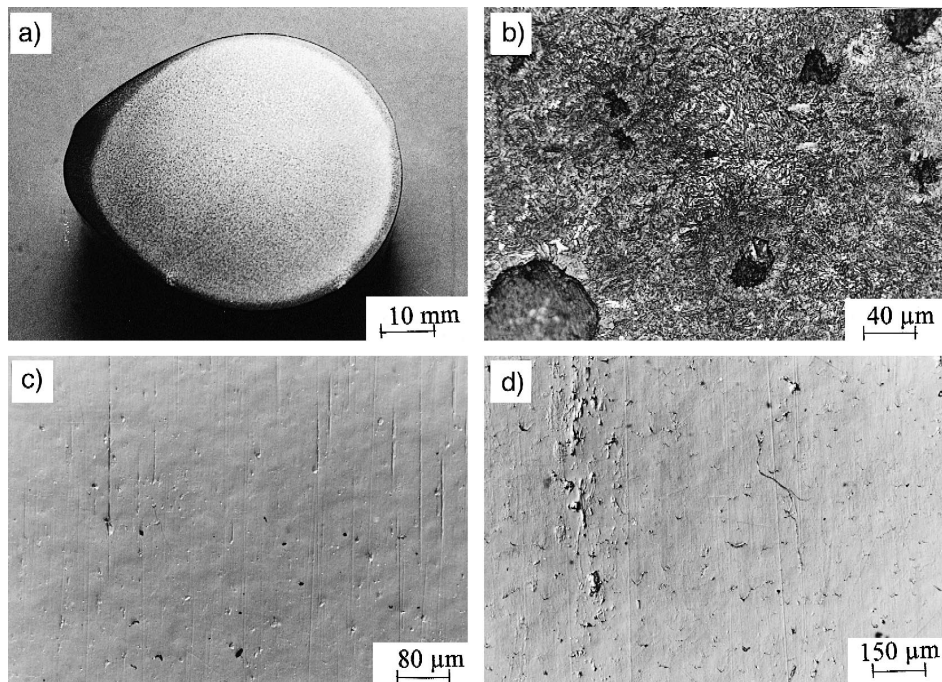


Fig. 8. Cam C1. Crosssection with a dark hardened layer on the circumference (a), hardened layer-nodular graphite, fine-acicular martensite (b), the surface of a cam flank with smooth abrasive wear (c), a strip of chippings and surface originated cracking on the shaft (d).

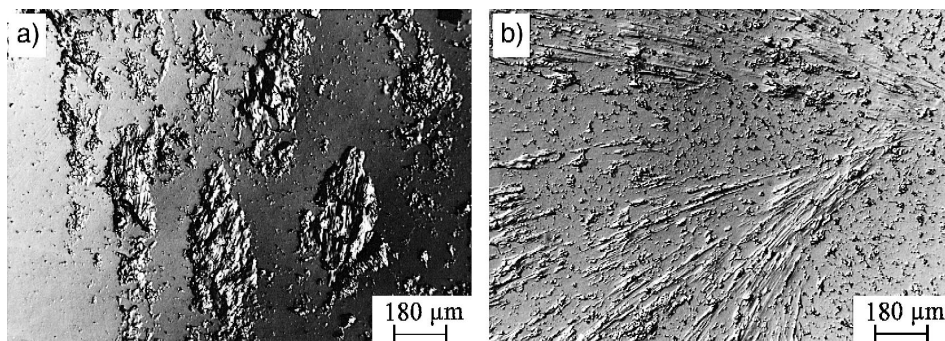


Fig. 10. Surfaces of cam 7 and follower F4. The lobe of the cam with metal fragments torn off the surface layer and chipped cementite particles (a), follower with cementite chippings and traces of surface deformation by hard particles (b).

### 5.2.2. Chilled cams of transformed ledeburite structure — steel followers of martensite structure with a layer formed by ion nitriding

Camshafts C8 and C9 were also made of grey, pearlite low-alloyed cast iron but they had a small extra amount of Mo, Ni and Cu hardening the cast iron and breaking up the structure. The core hardness was 272–286 HB. The internal negative stresses just below the surface area were –650 MPa. The surface layer was chilled while being cast. The hardness of the cam surface is 50–51 HRC. It contains transformed ledeburite without preeutectic pearlite inclusions. Valve followers F5 and F6 of 57–59 HRC (681–734 HV0.05) were made of 40H steel, which was quenched and tempered, surface hardened and ionitrided. The metallographic structure was martensite without the diffusion zone of nitriding. On the flank and lobe surfaces of the cams, there occurred smooth, abrasive wear without peelings, of small wear value (Table 5). The friction moment had the smallest value of the kinematic pairs under investigation. The face of the follower shows smooth abrasive wear. This material pair is recommended.

The wear value which was attained for the cams of camshaft C9 and followers F6 in the investigated combustion engine was slightly greater than that for the C8–F5 pair presented above (Table 5). The nature of the wear of cams C8, C9 and correspondingly, followers F5 and F6 was the same. The bench tests of the diesel engine reliability confirmed the correctness of the applied laboratory investigation of cams and valve followers.

## 6. Conclusions

The explanation of the results obtained for the cam–follower kinematic pair wear arises from the Hertzian theory as well as from the occurrence of tensile stresses at slide contact [20]. At contact points, tensile stresses behind the contact surface of the C2 nodular cast iron cam and the grey cast iron follower, hardened during casting, may have attained a value exceeding their tensile strength. Internal

stresses were also of tensile nature at small depths, which helped the process.

Ductile cast iron cams of martensite–bainite structure with a varied amount of retained austenite show a similar wear mechanism, considerable differences in wear intensity and different resistance values of their follower friction. Typical cam shapes after wear demonstrate that the attack side wears out more than the taper side. Cam overheating during induction hardening increases the thickness and hardness of the hardened layer, the amount of retained austenite, the depth at which internal stresses occur and changes their distribution pattern. After the work of the valve gear in the lobe part, cams C2 have numerous cavities due to metal chipping. On the other hand, the flank surfaces of the cams show numerous big and deep cracks in the surface layer metal. They run more or less perpendicularly to the direction of the sliding on the follower surface. The faces of the mating followers show a number of tear-outs and some delimitation wear on the surface and the cementite plates are broken. The formation of a nitrided layer on the hard and thick martensitobainitic matrix of cams C5 ensures its small radial wear. The cams undergo smooth abrasive wear. The followers also undergo smooth abrasive wear of a small value. Nitriding pearlitoferrite cast iron results in considerable wear of the C3 cams. Its disadvantage is that the depth of the hardened layer is much smaller than that of the impact of the stresses resulting from the kinematic pair load, the base being ductile. The use of sulfonitriding is a disadvantage despite further friction reduction. It causes a state of small compressive stress, which is unfavourable considering the tensile strength of the cams C4 and C6 surface.

Advantageous features are characterized in a camshaft made of grey pearlite low alloyed cast iron containing such elements as Mo, Ni and Cu, which harden cast iron and break up the structure. The camshaft is chilled during casting and has the structure of transformed ledeburite without preeutectic ferrite inclusions (casting with densifiers over the whole surface of the cams). Mating with a follower made of toughened, surface hardened and ioni-

trided steel ensures small frictional resistance and less abrasive wear with regard to tribologic wear. This material pair of the friction kinematic pair is recommended.

### Acknowledgements

The authors are grateful for the financial support provided by the Car Research and Development Centre (at present DAEWOO FSO) in Warsaw.

They also wish to thank Ms. H. Majka MSc and Eng. J. Biedroń for their help with retained austenite analyses.

### References

- [1] H.A. Rothbart, *Cams Design, Dynamics and Accuracy*, Wiley, New York, 1960.
- [2] P.C. Sui, T.Y. Torng, Cam/roller component fatigue reliability analysis (SAE 950708 Transactions), *Journal of Materials and Manufacturing* 104 (1995) 618–627, Section 5.
- [3] E. Kościelny, J. Michalski, The effect of the running dynamics of a direct valve-gear with a synthetic profile shaft on its wear. *Research Fascicles of Rzeszów University of Technology, Mechanics* 31 (12) (1986) 47–50, (in Polish).
- [4] C.M. Talyor, Automobile engine tribology — design considerations for efficiency and durability, *Wear* 221 (1) (1998) 1–8.
- [5] J.C. Bell, T.A. Cjogan, Critical physical conditions in the lubrication of automotive valve train system, *Tribology International* 24 (2) (1991) 77.
- [6] A.J. Black, E.M. Kopalinsky, P.L.B. Oxley, Sliding metallic wear test with in-process wear measurement: a new approach to collecting and applying wear data, *Wear* 200 (1996) 30–37.
- [7] P.D. Purmer, W. Van den Berg, Measurement of camshaft wear — wear and kinematics of overhead camshafts, *SAE Technical Paper Series* 850442.
- [8] J. Michalski, Synthetic profile cam and regulating plate wear in the direct valve-gear of a combustion engine, *Combustion Engines* 2 (1988) 1–8, (in Polish).
- [9] V. Zeman, *Materiály vackových hridelů*, *Automobil* 3 (1985) .
- [10] Ricardo Consulting Engineers, *Cam and follower materials*, Restricted DP 82/333, 1982.
- [11] British Technical Council of the Motor and Petroleum Industries, *Cams and Tappets, a Survey of Information*, Dec. 1972.
- [12] H. Müller, A. Kaiser, Composite camshaft — avoid lobe grinding using precision PM lobes (SAE 970001 Transactions), *Journal of Materials and Manufacturing* 106 (1997) 1–5, Section 5.
- [13] F. Reinke, Aufbau Ledeburitischer Randschichten durch Umschmelzbehandlung von Nocken und Nockenfolgern, *VDI-Berichte* 506 (1984) .
- [14] J.G. Heinrich, H. Krüner, Silicon nitride materials for engine applications, *cfi/Ber. DKG* 72 (4) (1995) 167–175.
- [15] V. Smith, B. Deckman, D. Brueck, Advanced ceramics: where do we go from here?, *Am. Ceram. Soc. Bull.* 73 (12) (1994) 49–52.
- [16] T. Tsujiuchi, K. Akas, Latest cam grinding technology — external or internal cams by using CBN superabrasives and CNC control (SAE 890980 Transactions), *Journal of Materials* 98 (1989) 831–851, Section 5.
- [17] Norm CEC L-38-A-94 — Gasoline engine valve train scuffing wear test (PSA TU3M/KDX engine).
- [18] Norm BN-79/1374-05 — Motor-car engines. Bench tests. Running-in.
- [19] Norm BN-79/1374-04 — Motor-car engines. Bench tests. Reliability tests.
- [20] D.F. Diao, K. Kato, K. Hayashi, The maximum tensile stress on a hard coating under sliding friction, *Tribology International* 27 (4) (1994) 267–272.

Dr. Jacek Michalski took his first degree at the Faculty of Mechanic Engineering and Aeronautics, Rzeszów University of Technology, and went on to obtain his Licentiate. His research interests are in manufacturing processes, measurement and tribology.

Dr. Józef Marszałek took his first degree at the Faculty of Ferrous Metals, Cracow Academy of Mining and Metallurgy, and went on to obtain his Licentiate. His research interests are in material analysis, tribology and fatigue wears.

Dr. Krzysztof Kubiak took his first degree at the Faculty of Non-ferrous Metals, Cracow Academy of Mining and Metallurgy, and went on to obtain his Licentiate. His research interests are in material analysis, constitution technical metals and plasticity deformation.